Heart and Vessels (2019) 34:1639–1649
https://doi.org/10.1007/s00380-019-01410-4

ORIGINAL ARTICLE

Impact of neointimal tissue characterization and heterogeneity of bare-metal stents and drug-eluting stents on the time course after stent implantation evaluated by integrated backscatter intravascular ultrasound

Takashi Yoshizane[1] · Shinichiro Tanaka[2] · Shintaro Abe[1] · Takahiro Ueno[1] · Yoshiaki Goto[1] · Tai Kojima[1] · Makoto Iwama[1] · Masazumi Arai[1] · Toshiyuki Noda[1] · Masanori Kawasaki[3]

Received: 25 December 2018 / Accepted: 12 April 2019 / Published online: 17 April 2019

Abstract

Pathological studies have suggested the different process of in-stent restenosis (ISR) of bare-metal stents (BMS) and drug-eluting stents (DES). Here, we evaluated the components of neointimal tissue using integrated backscatter intravascular ultrasound (IB-IVUS) and focused on the time course after stent implantation and tissue signal distribution. We evaluated 125 lesions of 125 patients who underwent target lesion revascularization for ISR (BMS: $n=73$, DES: $n=52$). Volume analysis of a 4-mm length centered on a minimum lumen area in every 1-mm cross-sectional area was performed. For IB-IVUS analysis, color-coded maps were constructed from the default setting based on the integrated backscatter (IB) values (middle-IB value, green: fibrous and low-IB value, blue: lipid pool). For the neointimal tissue volume, we evaluated the ratios of the green (%G) and blue (%B) areas. Tissue signal distribution (TD) was also obtained from the default setting based on IB values in each pixel of IB-IVUS imaging. We compared values of neointimal tissues measured by IB-IVUS between the DES and BMS and time course. The observed period was longer after BMS implantation than after DES implantation (BMS: 2545 days, DES: 1233 days, $p<0.001$). Overall, %G and %B were similar between the BMS and DES groups (%G: 55% and 51%, respectively, $p=0.10$; %B: 36% and 38%, respectively, $p=0.51$); however, TD was significantly higher in the DES group than in the BMS group (1091 vs. 1367, $p<0.001$). TD in the DES group remained high during the follow-up periods. However, TD in the BMS group was low in the early phase and significantly increased over time ($r=0.56$, $p<0.001$). When analyzing the ISR within 2 years after stent implantation, the BMS was distinguished with a sensitivity of 66% and a specificity of 90% (cut-off value: TD = 1135, area under the curve 0.83, 95% confidence interval 0.74–0.92). TD could differentiate neointimal tissue after BMS implantation in the early phase. TD can be a useful index in the observation of neoatherosclerosis.

Keywords Neoatherosclerosis · Tissue signal distribution · Integrated backscatter intravascular ultrasound · Bare-metal stent · Drug-eluting stent

Introduction

Coronary stent implantation is a standard therapy for percutaneous coronary intervention (PCI). Although drug-eluting stents (DES) reduce neointimal proliferation compared to bare-metal stents (BMS) in the early phase, concerns remain about the atherosclerotic change pathologically in the neointimal tissue of patients with DES and BMS in the late phase [1]. These concerns have led to a different mechanism of coronary response between DES and BMS or different periods after stent implantation according to the time course. A pathological study reported that earlier neoatherosclerotic

✉ Takashi Yoshizane
takashiyoshizane@gmail.com

[1] Department of Cardiology, Gifu Prefectural General Medical Center, 4-6-1, Noishiki, Gifu 500-8226, Gifu, Japan

[2] Asahi University Hospital, Gifu, Gifu, Japan

[3] Gifu University Graduate School of Medicine, Gifu, Gifu, Japan

change occurs with the DES and that neoatherosclerotic change occurred only beyond 2 years with BMS [2].

Integrated backscatter intravascular ultrasound (IB-IVUS) is a useful method for analyzing coronary plaque tissue [3–5]. Earlier reports suggested that color-mapping imaging provided by IB-IVUS can be used to assess neointimal tissue patterns; BMS restenosis in the early phase was represented by a homogeneous pattern; on the other hand, neoatheroscleosis was represented by a heterogeneous pattern [6]. However, quantitative evaluation was limited, because distinguishing smooth muscle cells within neointimal tissue from other tissue types using IB-IVUS were difficult. Neointimal tissue is not strictly clarified by IB-IVUS; however, this modality can provide integrated backscatter (IB)-related values by a default setting derived from the average power of backscatter radiofrequency signals. We wondered whether these IB-related values are associated with the neointimal pattern. Therefore, this study aimed to evaluate the components of neointimal tissue with DES and BMS implantation using IB-IVUS by focusing on the time course after stent implantation and the tissue heterogeneity-derived IB-related value.

Materials and methods

The present study was conducted according to the principles of the Declaration of Helsinki and was approved by the Ethics Committee of Gifu Prefectural General Medical Center. All study participants gave informed consent for study enrollment.

Study design and eligibility

This retrospective study included patients who had received PCI for target lesion revascularization (TLR) with IB-IVUS. Follow-up angiography after stent implantation was performed 1 or 2 years after coronary stent implantation in Gifu Prefectural General Medical Center. Reasons for unplanned follow-up angiography or a follow-up period of more than 2 years were as follows: (1) recurrent stable angina; (2) evidence of silent myocardial ischemia, such as an electrocardiographic change and nuclear stress test abnormality; or (3) planned follow-up angiography for another stent segment. Patients with acute myocardial infarction due to ISR, those having any thrombi in their coronary arteries, and those in whom the vascular lesion was in a coronary artery bypass graft were excluded to avoid bias of the IB values of the thrombus as much as possible. We also excluded patients with lesions with stent edge restenosis and those treated with TLR previously. In addition, we excluded patients whose IVUS images were too poor to analyze. From 2012 to 2016, we performed 1602 elective PCIs (322 cases of ISR), and 125 lesions of 125 patients fulfilled these criteria.

IB-IVUS procedure and data

The IVUS procedure and data acquired were referred to in previous reports [3, 7]. IVUS examinations for ISR lesions were performed before any intervention. The transducer was advanced into the distal side of the target lesion, and an imaging run was performed back through the stent to the coronary ostium using a motorized transducer auto-pullback system (0.5 mm/s). Ultrasound backscattered signals were acquired with a commercially available IVUS imaging system (VISIWAVE, Terumo, Tokyo, Japan) using a 40-MHz rotating IVUS catheter (View it, Terumo). All IVUS imaging data were transferred to a personal computer equipped with the custom software (VISIATLAS, Terumo). Tissue characterization of the neointimal composition was achieved with IB-IVUS using VISIATLAS. Cross-sectional images were obtained as 1-mm slices of the stent, and IB-IVUS color-coded maps could be displayed by tracing the vessel area, lumen area, and stent area. Neointimal tissue was defined as the area between the lumen border and the inner border of the stent struts to avoid stent strut artifacts. Furthermore, the guidewire was removed to avoid guidewire artifacts and severe calcification, and its dorsal parts were removed to avoid the effect of the shadow attenuation phenomenon caused by calcification (Fig. 1). We applied the manufacturer's default settings based on previous data [3–5, 8] to define a range of IB values for neointimal tissue components. Representative color-coded maps of cross-sectional coronary artery plaques were constructed using IB cut-off points to discriminate calcification (red, IB value < -29 dB), fibrosis (green, -49 dB $\leq$ IB value < -29 dB), and lipid pool (blue, -49 dB $\leq$ IB value), as described previously [3, 7].

Volume analysis of a 4-mm length centered on the minimum lumen area of ISR for every 1-mm cross-sectional area (CSA) was performed, and each CSA at 1-mm slices was interpolated and integrated (Fig. 1). As a reason for that there were many cases in which neointimal proliferation was located in the focal segment, and the neointimal area could not be measured from the whole stent segment in cases of DES restenosis. We calculated the stent volume, lumen volume, neointimal tissue volume (stent volume − lumen volume), and each component of the neointimal tissue volume, and we obtained the % volume of green (%G = volume of green/neointimal tissue volume) and % volume of blue (%B = volume of blue/neointimal tissue volume). The rendering of the color mapping in the IB-IVUS system was constructed by dividing a series of IB values obtained from the radiofrequency signal into 256 classes as original values, so-called "color values," in each pixel of every CSA (Xi: color value of the pixel in neointimal tissue). From this

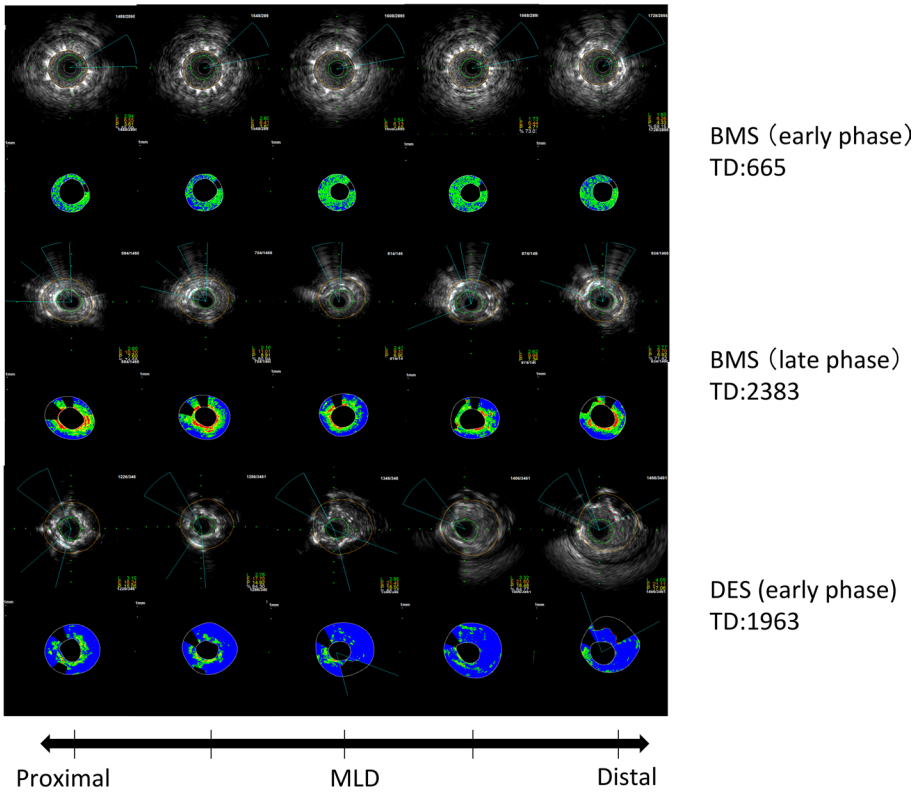

Fig. 1 Representative images of intravascular ultrasound. *TD* tissue signal distribution, *BMS* bare-metal stents, *DES* drug-eluting stents

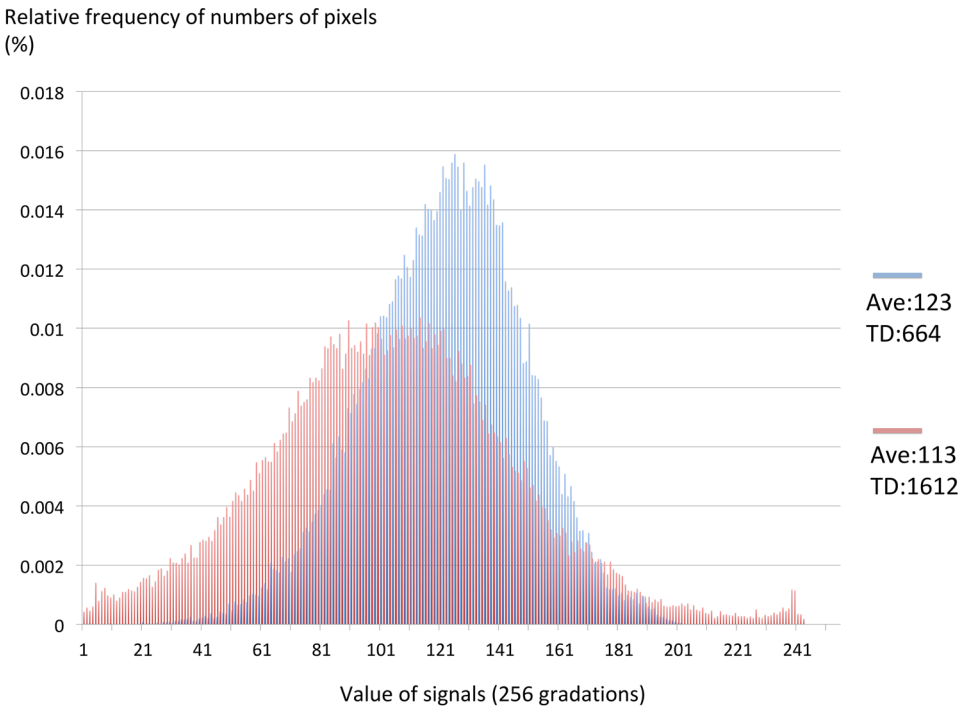

Fig. 2 Representative images of distributions of signals in neointimal tissues; graph of blue lines, which analyzed the early stage of BMS, showed low TD (TD: 664, ave: 123), in contrast, graph of red lines, which analyzed DES, showed high TD (TD: 1614, ave: 113). *BMS* bare-metal stent, *TD* tissue signal distribution, *Ave* average value of signals, *DES* drug-eluting stent

default setting, the average value (Av: average color value of neointimal tissue) and variance (unbiased tissue signal distribution) can be automatically obtained for this original number for each CSA using the IB-IVUS system. Tissue signal distribution (TD) was defined as the average variance of the observed CSAs, meaning that the low value of TD was homogeneous or that the high value was heterogeneous (Fig. 2). The formula used to calculate TD by the default

setting in VISIATLAS is as follows: variance (TD) = $S^2 = \Sigma^n{}_1(\mathrm{Xi} - \mathrm{Av})^2/n - 1$, where n is the number of pixels in neointimal tissue.

We evaluated the time course changes of neointimal tissue. In addition, we compared the IB-IVUS parameters in the early phase (< 2 years after stent implantation) and late phase (> 2 years after stent implantation).

Statistical analysis

Continuous data are expressed as means ± standard deviations (SD) or medians and interquartile range (IQR), and categorical data are expressed as frequencies or percentages. Continuous variables were compared using the *t* test or Mann–Whitney *U* test. Categorical variables were compared using the Fisher exact test. The relationship among several parameters obtained by IB-IVUS and the time after stent implantation was analyzed by simple linear regression analysis. The receiver operating characteristics (ROC) curve was used to determine the optimal cut-off values and the sensitivity and specificity of the IB-IVUS parameters to predict neoatherosclerosis within 2 years after BMS implantation. Pathological neoatheromatic change was rare within 2 years after BMS implantation and led to the prediction of pathological neointimal hyperplasia or neoatherosclerosis [2].

All analyses were performed using Excel (Microsoft Corp., Redmond, WA, U.S.A.) and EZR (Saitama Medical Center, Jichi Medical University, Saitama, Japan). EZR is a graphical user interface for R (The R Foundation for Statistical Computing, Vienna, Austria); more precisely, it is a modified version of R commander designed to add statistical functions used in biostatistics [9]. Values of $p < 0.05$ were considered significant.

Results

Characteristics of the study population

The clinical characteristics of the study participants are shown in Table 1. The average observation period after stent implantation was 1999 days, and the period was longer after BMS implantation than after DES implantation (2545 days and 1233 days, respectively; $p < 0.001$). Patients' mean age was 70 years, 81% of patients were men, 78% had hypertension, 69% had hyperlipidemia, 51% had diabetes, 33% smoked, and 14% were on hemodialysis. Among these aforementioned variables, a significant difference was only seen in hemodialysis between the BMS and DES groups (8% vs. 22%, $p = 0.027$). Target lesions were localized in the left anterior descending artery in 57 patients (46%), left circumflex artery in 15 (12%), and right coronary artery in 50 (42%). There was no significant difference in stent length between the groups (BMS: 21.3 mm, DES: 22.4 mm).

Participants' medications are also summarized in Table 1. There were no significant differences in medications between the two groups. Under these medical treatments, the mean total cholesterol level was 169 mg/dl, triglyceride level was 149 mg/dl, high-density lipoprotein cholesterol level was 49 mg/dl, low-density lipoprotein cholesterol level was 91 mg/dl, and glycated hemoglobin A1c level (according to the NGSP) was 6.3%. In addition, the mean serum creatinine level was 1.8 mg/dl, and left ventricular ejection fraction determined by echocardiography was 58.7%. Among these aforementioned variables, a significant difference was only seen in the serum creatinine level between the BMS and DES groups (1.4 mg/dl vs. 2.3 mg/dl, $p = 0.031$). However, serum creatinine level had a lot of outliers from the mean and it was a non-normal distribution, so we expressed serum creatinine level as median (IQR) and applied the Mann–Whitney *U* test, the result of which showed no significant differences between BMS and DES (0.9 mg/dl vs. 1.0 mg/dl, $p = 0.065$).

Conventional and IB-IVUS analyses

The results of quantitative and qualitative analyses using IB-IVUS of the entire stent are shown in Table 2. In the quantitative analysis, the average stent volume and average total neointimal tissue volume were 31.5 and 17.3 mm^3, respectively. The stent volume and plaque volume were larger in the BMS group than in the DES group (stent volume: 33 and 30 mm^3, respectively; $p = 0.022$; neointimal tissue volume: 18 and 16 mm^3, respectively; $p = 0.028$). In the qualitative analysis, the neointimal volume of the green area and its ratio (%G) were larger in the BMS group than in the DES group (volume of green: 9.9 and 7.8 mm^3, respectively, $p = 0.003$; %G: 55% and DES 51%, respectively, $p = 0.098$). However, there were no significant differences in the neointimal tissue volume of the blue area and its ratio (%B) between the groups. Tissue signal average showed no significant difference between the groups; on the other hand, TD was significantly smaller in the BMS group than in the DES group (1090 vs. 1367, $p < 0.001$).

Time-course changes of neointimal tissue

In Table 3 and Fig. 3, only TD of the BMS group showed a significant difference between the early and late phases (856 vs. 1220, $p < 0.001$). In addition, only TD in the early phase showed a significant difference between the BMS and DES groups (856 vs. 1423, $p < 0.001$). Scatter plots comparing %G, %B, and TD over time after stent implantation are shown in Fig. 4. No significant difference was observed in the changes of green and blue plaque volumes over time. In

Table 1 Patient characteristics

Patient characteristics	Total ($n=123$)	BMS ($n=72$)	DES ($n=51$)	p value
Days after stent implantation (days)	1999 ± 1830	2545 ± 1990	1233 ± 1234	< 0.001
Sex, me n = n (%)	100 (81%)	60 (83%)	40 (78%)	0.493
Age (years)	69.8 ± 8.9	69.0 ± 9.4	70.9 ± 8.2	0.260
Body mass index (%)	24.3 ± 3.2	24.6 ± 3.1	23.8 ± 3.3	0.137
Past history				
Hypertension	96 (78%)	54 (75%)	42 (82%)	0.382
Hyperlipidemia	85 (69%)	52 (72%)	33 (65%)	0.430
Diabetes mellitus	63 (51%)	32 (44%)	31 (61%)	0.067
Smoker	41 (33%)	19 (26%)	22 (43%)	0.054
On HD	17 (14%)	6 (8%)	11 (22%)	0.027
Stent information				
Stent length (mm)	21.8 ± 6.7	21.3 ± 6.0	22.4 ± 7.5	0.381
Types of drug-eluting stent				
Sirolimus	–	–	14 (19%)	–
Paclitaxel	–	–	3 (4%)	–
Zotarolimus	–	–	5 (7%)	–
Everolimus	–	–	30 (42%)	–
Affected vessels				
Left anterior descending	57 (46%)	31 (43%)	26 (51%)	
Left circumflex	15 (12%)	11 (15%)	4 (8%)	
Right	50 (41%)	29 (40%)	21 (41%)	
Medications (during hospitalization)				
Aspirin	120 (98%)	70 (97%)	50 (98%)	N/A
Thienopyridine	25 (20%)	13 (18%)	12 (24%)	0.500
Clopidogrel	89 (72%)	53 (74%)	36 (71%)	0.838
Plusgrel	3 (2%)	1 (1%)	2 (2%)	0.569
Cilostazol	8 (7%)	4 (6%)	4 (8%)	0.717
Warfarin	12 (10%)	10 (14%)	2 (4%)	0.120
ACE-I/ARB	84 (68%)	48 (67%)	36 (71%)	0.697
Beta blocker	57 (46%)	35 (49%)	22 (43%)	0.586
Statin	88 (72%)	56 (78%)	32 (63%)	0.104
Calcium channel blocker	61 (50%)	33 (46%)	28 (55%)	0.363
Diuretics	32 (26%)	15 (21%)	17 (33%)	0.146
Laboratory data				
Creatinine (mg/dl)	0.9 (0.7–1.2)	0.9 (0.7–1.1)	1.0 (0.8–2.0)	0.065
HbA1c (NGSP) (%)	6.3 ± 0.8	6.2 ± 0.8	6.4 ± 0.9	0.427
Total cholesterol (mg/ dl)	169.0 ± 36.4	171.6 ± 32.7	165.3 ± 41.1	0.346
Triglyceride (mg/ dl)	148.9 ± 76.0	157.4 ± 80.5	136.8 ± 68.2	0.137
HDL cholesterol (mg/ dl)	48.7 ± 11.9	48.4 ± 11.9	49.2 ± 11.9	0.702
LDL cholesterol (mg/ dl)	91.3 ± 31.3	92.4 ± 29.0	89.2 ± 34.5	0.649
Echo parameter				
LVEF (%)	58.7 ± 10.6	59.3 ± 9.4	57.8 ± 12.2	0.443

Data are expressed as n (%) and mean (SD). Creatinine was expressed as median (IQR) because of a lot of outliers from the mean

HD hemodialysis, *ACE-I* angiotensin-converting enzyme inhibitor, *ARB* angiotensin2 receptor blocker, *HbA1c* hemoglobin A1c, *NGSP* National Glycohemoglobin Standardization Program, *HDL* high density lipoprotein, *LDL* low density lipoprotein, *LVEF* left ventricular ejection fraction

contrast, a significant difference was observed in the change of TD of the BMS group, which was low in the early period and increased over time (correlation: 0.56, 95% confidence interval: 0.38–0.70, $p<0.001$). TD of the DES group tended to be high from the early period, but it did not change significantly over the long-term follow-up ($p=0.346$). The

Table 2 Conventional IVUS data and IB-IVUS data

Patient characteristics	Total ($n=123$)	BMS ($n=72$)	DES ($n=51$)	p value
Volume analysis				
Luminal volume (mm^3)	14.2 ± 4.2	14.5 ± 4.6	13.8 ± 3.7	0.357
Stent volume (mm^3)	31.5 ± 8.1	32.9 ± 8.0	29.6 ± 7.8	0.022
Neointimal tissue volume (mm^3)	17.3 ± 6.6	18.4 ± 6.6	15.8 ± 6.3	0.028
IB-IVUS analysis				
Volume of green (mm^3)	9.0 ± 4.0	9.9 ± 4.1	7.8 ± 3.7	0.003
Volume of blue (mm^3)	6.7 ± 5.5	7.0 ± 5.7	6.3 ± 5.2	0.496
%Volume of green (%)	53.3 ± 15.4	55.2 ± 16.4	50.6 ± 13.7	0.098
%Volume of blue (%)	36.8 ± 19.7	35.8 ± 20.6	38.1 ± 18.4	0.512
Tissue signal average	129.5 ± 19.7	131.5 ± 19.7	126.7 ± 19.6	0.179
Tissue signal distribution	1205.8 ± 374.3	1090.8 ± 325.7	1367.3 ± 381.4	< 0.001

IB integrated backscatter, *IVUS* intravascular ultrasound, *BMS* bare-metal stent, *DES* drug-eluting stents

Table 3 IB-IVUS date, early phase (< 2 years), or late phase (≥ 2 years)

	BMS			DES			p*1	p*2
	Early	Late	p	Early	Late	p		
% Volume of green (%)	58.0 ± 16.4	53.6 ± 15.6	0.277	50.7 ± 14.2	50.4 ± 13.5	0.937	0.116	0.368
% Volume of blue (%)	35.7 ± 21.3	35.8 ± 20.5	0.996	37.2 ± 18.8	38.9 ± 18.3	0.736	0.803	0.505
Tissue signal average	131.5 ± 18.9	131.5 ± 20.4	0.993	127.3 ± 20.4	126.1 ± 19.2	0.331	0.820	0.259
Tissue signal distribution	856.2 ± 179.4	1220.6 ± 316.5	< 0.001	1423.4 ± 472.8	1319.2 ± 281.3	0.331	< 0.001	0.179

IB integrated backscatter, *IVUS* intravascular ultrasound, *BMS* bare-metal stent, *DES* drug-eluting stents

*1: Early restenosis BMS vs. DES

*2: Late restenosis BMS vs. DES

difference between TD of the BMS and DES groups is clearly shown in Fig. 4.

Prediction of neoatherosclerosis 2 years after BMS implantation

Sensitivity and specificity of IB-IVUS parameters to predict BMS within 2 years after stent implantation, which indicated neointimal hyperplasia, because neoatheromatic change was rare within 2 years after BMS implantation, are shown in Fig. 5. The area under the curve was higher for TD than for any other parameters, so it may be considered as the most accurate predictor of neoatherosclerosis (area under the curve: 0.83, cut-off value: 1135, sensitivity: 66%, specificity: 90%).

Discussion

In the present study, there were significant differences between stent types (BMS and DES) and follow-up periods (early phase and late phase), but %G and %B were not significantly different between the stent types and follow-up periods. In addition, TD was a superior indicator of neointimal tissue change in the early phase after BMS implantation.

Herein, TD was low in the neointimal tissue of patients with BMS in the early phase. TD was variance of color index for contracted color mapping. When TD became lower, the color mapping became homogeneous. It is well known that neointimal hyperplasia was consisted of smooth muscle cells in proteoglycan and the collagen matrix, so neointimal hyperplasia with BMS in the early phase is represented by a homogeneous pattern [2, 7]. Those previous study findings support our study results that TD was low in the neointimal tissue in the early phase after BMS implantation. Although a homogeneous or heterogeneous pattern detected by IB-IVUS can indicate the ISR pattern, this visual pattern may lack objectivity and quantitative merit. A previous pathological study showed that intimal hyperplasia with BMS in the early phases produced IB values similar to the lipid pool and the same color-coded mapping [3]; however, in a clinical study, neointimal hyperplasia was classified as fibrous based on color mapping [2, 7, 10]. Although it was speculated that the IB value is unknown or wide in pathological components, such as actin levels in smooth muscle cell, the extracellular matrix, and thrombus [7], this controversy remains unclear. In clinical practice, physicians should pay attention to the

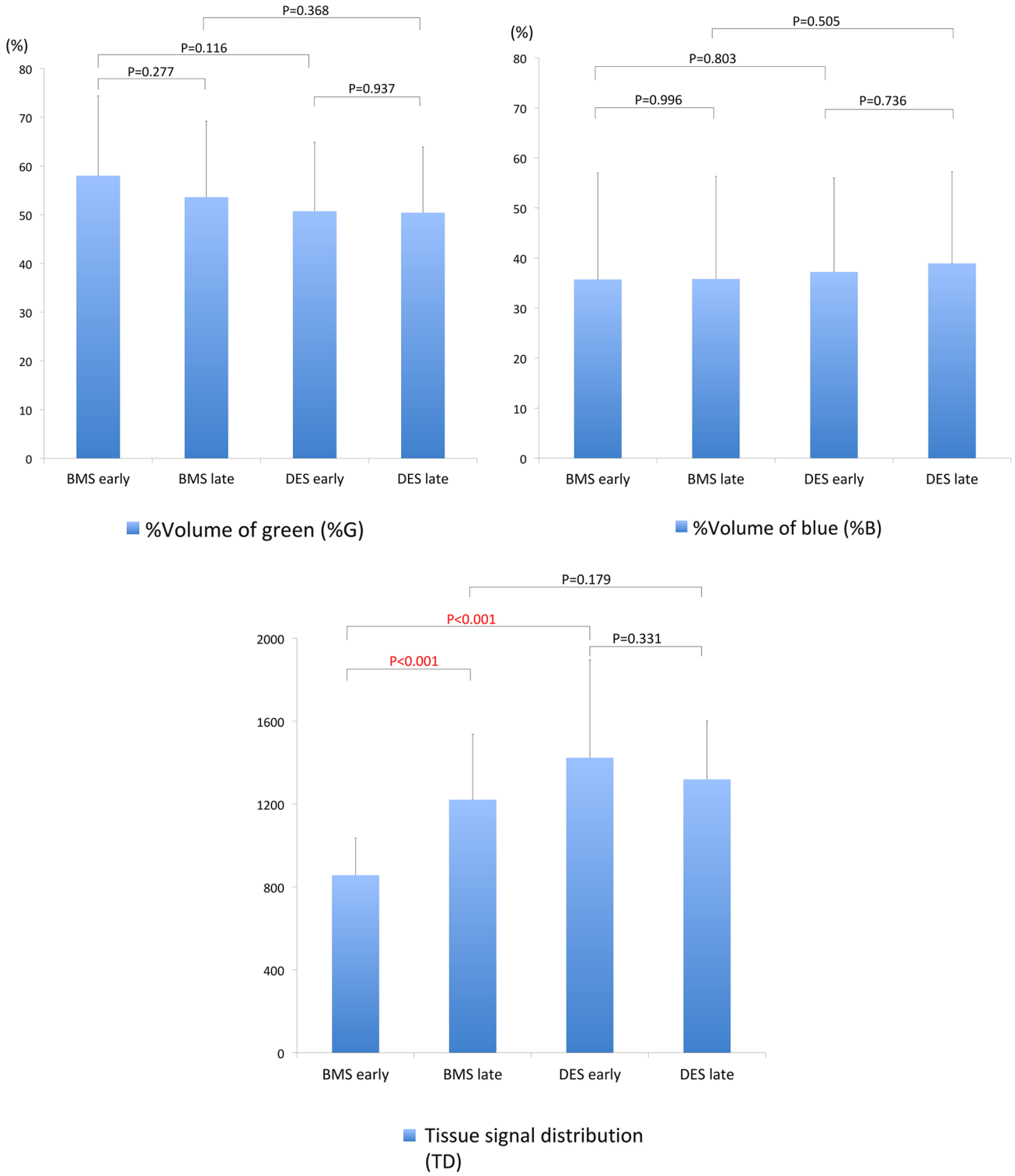

Fig. 3 Comparison of neointimal tissue components and tissue signal distribution between BMS and DES, and between the early phase (within 2 years after stent implantation) and late phase (2 years after stent implantation). 2–1: % volume of the green area (%G); 2–2: % volume of the blue area (%B); 2–3: tissue signal distribution (TD). *BMS* bare-metal stents, *DES* drug-eluting stents

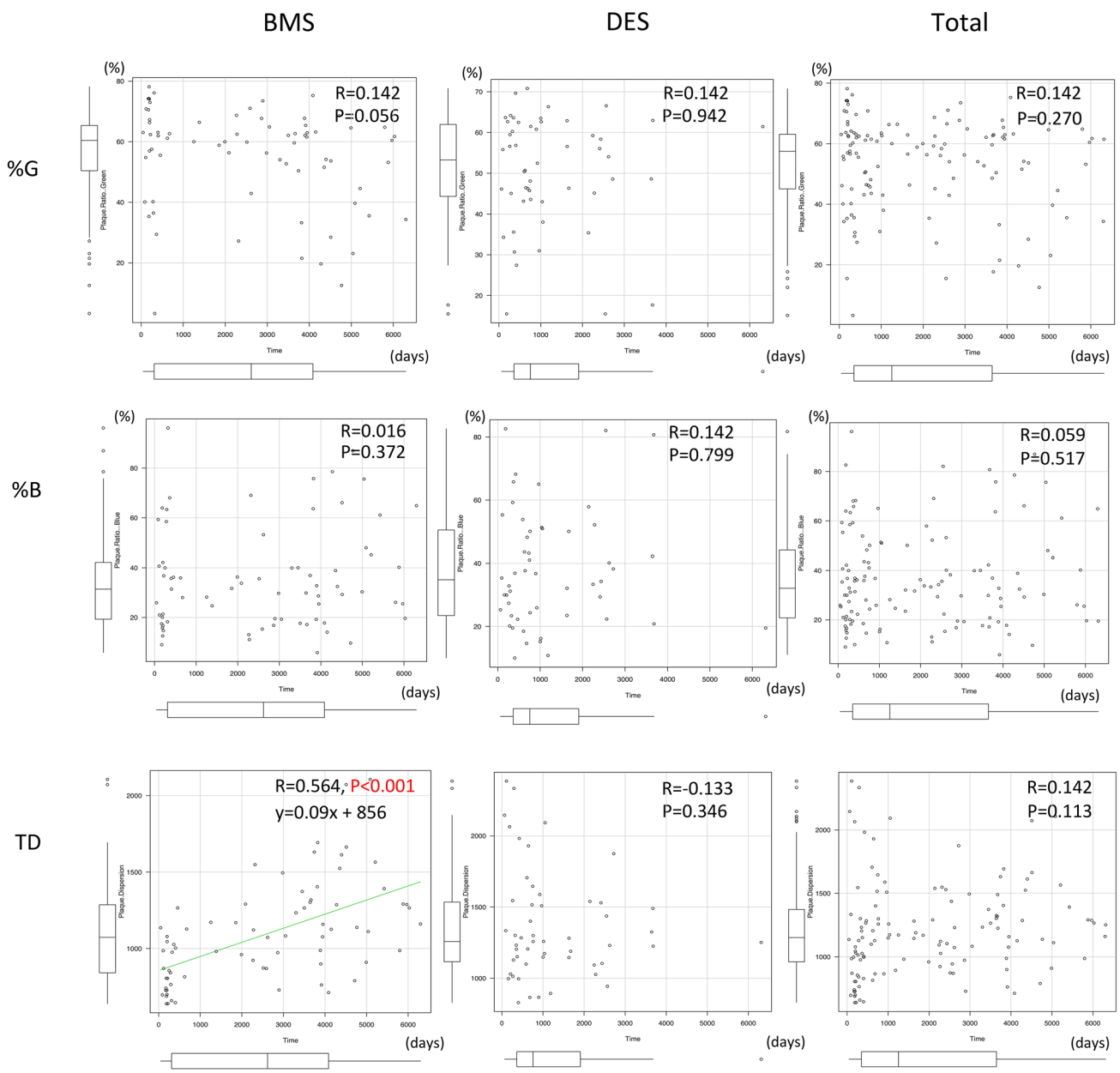

Fig. 4 Time courses of the ratio of neointimal tissue volumes and TD in the subgroups (BMS, DES, and overall). The relationships were evaluated by simple regression analysis. *%G* the ratio of the volume of the green area, *%B* the ratio of the volume of the blue area, *TD* tissue signal distribution, *BMS* bare-metal stent, *DES* drug-eluting stent

pathological accuracy and physical characteristics obtained from radiofrequency signals, such as IB values, which might easily lead to a homogeneous or heterogeneous pattern. TD can be easily obtained from the default setting of IB-IVUS. A homogeneous or heterogeneous pattern can lead to misclassification of the color-coded classification, for example, when IB values above the pathological components are near the cut-off value for native atherosclerosis criteria. TD-related IB values could be concern about the homogeneous or heterogeneous pattern rather than color mapping.

Different from the previous reports, the ratio of the tissue component according to native atherosclerosis criteria (%G and %B) was not significantly different between the DES group and BMS group, and over time. Previous reports showed that BMS implantation increased the % lipid area per volume (%B) or that DES implantation increased or maintained the % fibrous (%G) during the follow-up [2, 7, 10]. The reason for these findings may be the intrinsic limitation in evaluating neointimal tissue by IB-IVUS as aforementioned. Neointimal tissue growth involved a different

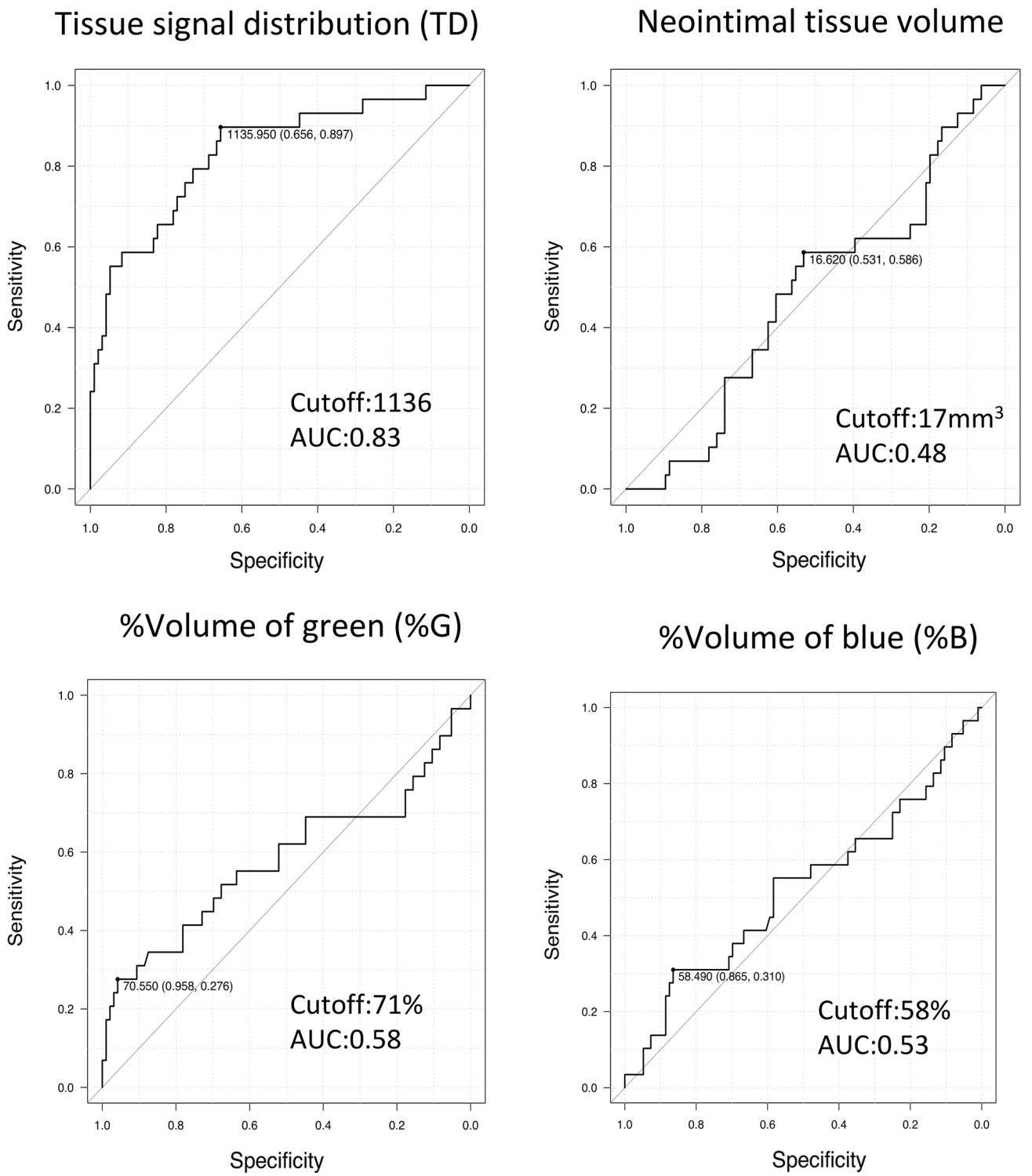

Fig. 5 Receiver operating characteristic curve for TD, the neointimal tissue volume, %G, and %B to predict BMS within 2 years after stent implantation. *TD* tissue signal distribution, *%G* the ratio of the volume of the green area, *%B* the ratio of the volume of the blue area, *BMS* bare-metal stent, *AUC* area under the curve

process, such as smooth muscle cell proliferation or neoatherosclerosis in various stages, which could be indicated as various IB color codes. Actually, a previous study found that %G and %B of neointimal tissue were significantly different between the early phase and late phase with BMS or DES, albeit these differences were weak [10]. Another

reason for our finding is that our study population included many patients with chronic kidney disease, including those receiving hemodialysis. Chronic kidney disease is one of the predictors of neoatherosclerosis, which results from incomplete endothelialization [11, 12]. However, we could not clearly show the relevance of chronic kidney disease in our study. When analyzing the correlation between serum creatinine level and TD, we found a weak correlation ($r=0.387$) as a whole; however, when the patients of hemodialysis were excluded, we could find no correlation between them ($r=0.197$). Further study and validation of neointimal tissue analysis is needed using specific histological classification for IB-related parameters and conventional color mapping. Currently, it is important to evaluate the physical characteristics obtained from radiofrequency signals.

Clinical implications

Our findings have important clinical implications. TD derived by IB-IVUS demonstrated in the present study could be used to distinguish neointimal hyperplasia or neoatherosclerosis. Physicians should try to use intensive medical therapy and vigorous lifestyle modification in patients after stent implantation to reduce the development of neoatherosclerosis [11]. Furthermore, IB-IVUS was useful for predicting the distal slow flow phenomenon after revascularization for ISR lesions [13]. Thus, the assessment of TD by IB-IVUS during PCI may provide physicians with useful information regarding the risk stratification of patients with coronary heart disease. Recently, it has been recommended to conduct IVUS during PCI [14], and in addition, we should also confirm IB-IVUS to get more detailed information like TD.

Limitations

This study had a retrospective, non-randomized design, the study population was small, and the results reflect the experience at only a single center. Therefore, it lacks the obvious advantages of a larger, multicenter, multinational randomized study. In addition, because the number of cases of DES was very small, comparing with the DES group was difficult. Previous studies reported that there was a pathological difference among each DES [15, 16], so further study on this topic is required.

We performed IB-IVUS at only one timepoint in a retrospective manner and did not sequentially perform IB-IVUS in each case. Hence, this study evaluated the different timepoint groups consisting of different cases and estimated the time course indirectly, and there were unknown or unmeasurable factors that could potentially alter the responses at other times.

At present, equipment with newly developed custom software is connected to the IVUS imaging system (VISICUVE, Terumo), and the histological cut-off points are different [8]. IB values and pathological evaluation of smooth muscle cells, in-vivo histopathologic characteristics of in-stent restenosis, were clarified with only the conventional IB-IVUS system [1]. It is necessary to perform further histopathological study to clarify the relationship between neointimal tissue and IB values.

Finally, as mentioned in method, this study excluded calcification. In quantifying TD values, calcification had to be excluded, because the impact of calcification itself and its back-attenuation on the dorsal side strongly influences the analysis. Coronary arteries of patients of hemodialysis are easy to be calcified and its restenosis rate is high [17]. Calcification is one of the most important factors that promote restenosis and it may be affect TD. Excluding calcification is considered to be the major limitation of this research.

In conclusion, TD from IB-IVUS clearly showed that the neointima of BMS was homogeneous in early periods and gradually became heterogeneous; on the other hand, the neointima of DES was already heterogeneous in the early periods, which suggested neoatherosclerosis. Since TD can quantify neoatherosclerosis, it may be a useful index in the observation of neoatherosclerosis in ISR.

Acknowledgements The authors would like to thank Yoshitake Oshima, MD; Syuntaro Horio, MD; Ryota Watanabe, MD; Hiroto Yagasaki, MD; Hirotaka Miwa, MD; Takashi Kato, MD; Syunichiro Warita, MD, PhD; Koji Ono, MD, PhD; and Shintaro Tanihata, MD, PhD for providing assistance in manuscript preparation.

Compliance with ethical standards

Conflict of interest The authors declare that they have no conflict of interest.

Ethics approval All procedures performed in studies involving human participants were in accordance with the ethical standards of the institutional and/or national research committee and with the 1964 Helsinki declaration and its later amendments or comparable ethical standards.

Informed consent Informed consent was obtained from all individual participants included in the study.

References

1. Nakazawa G, Otsuka F, Nakano M, Vorpahl M, Yazdani SK, Ladich E, Kolodgie FD, Finn AV, Virmani R (2011) The pathology of neoatherosclerosis in human coronary implants bare-metal and drug-eluting stents. J Am Coll Cardiol 57:1314–1322
2. Nakazawa G, Vorpahl M, Finn AV, Narula J, Virmani R (2009) One step forward and two steps back with drug-eluting-stents: from preventing restenosis to causing late thrombosis and nouveau atherosclerosis. JACC Cardiovasc Imaging 2:625–628

3. Kawasaki M, Takatsu H, Noda T, Sano K, Ito Y, Hayakawa K, Tsuchiya K, Arai M, Nishigaki K, Takemura G, Minatoguchi S, Fujiwara T, Fujiwara H (2002) In vivo quantitative tissue characterization of human coronary arterial plaques by use of integrated backscatter intravascular ultrasound and comparison with angioscopic findings. Circulation 105:2487–2492
4. Okubo M, Kawasaki M, Ishihara Y, Takeyama U, Kubota T, Yamaki T, Ojio S, Nishigaki K, Takemura G, Saio M, Takami T, Minatoguchi S, Fujiwara H (2008) Development of integrated backscatter intravascular ultrasound for tissue characterization of coronary plaques. Ultrasound Med Biol 34:655–663
5. Okubo M, Kawasaki M, Ishihara Y, Takeyama U, Yasuda S, Kubota T, Tanaka S, Yamaki T, Ojio S, Nishigaki K, Takemura G, Saio M, Takami T, Fujiwara H, Minatoguchi S (2008) Tissue characterization of coronary plaques: comparison of integrated backscatter intravascular ultrasound with virtual histology intravascular ultrasound. Circ J 72:1631–1639
6. Sato K, Costopoulos C, Takebayashi H, Naganuma T, Miyazaki T, Goto K, Yamane H, Hagikura A, Kikuta Y, Taniguchi M, Hiramatsu S, Ito H, Colombo A, Haruta S (2014) The role of integrated backscatter intravascular ultrasound in characterizing bare metal and drug-eluting stent restenotic neointima as compared to optical coherence tomography. J Cardiol 64:488–495
7. Tanaka S, Noda T, Iwama M, Tanihata S, Kawasaki M, Nishigaki K, Minagawa T, Watanabe S, Minatoguchi S (2013) Long-term changes in neointimal hyperplasia following implantation of bare metal stents assessed by integrated backscatter intravascular ultrasound. Heart Vessels 28:415–423
8. Kawasaki M, Hattori A, Ishihara Y, Okubo M, Nishigaki K, Takemura G, Saio M, Takami T, Minatoguchi S (2010) Tissue characterization of coronary plaques and assessment of thickness of fibrous cap using integrated backscatter intravascular ultrasound. Comparison with histology and optical coherence tomography. Circ J 74:2641–2648
9. Kanda Y (2013) Investigation of the freely available easy-to-use software 'EZR' for medical statistics. Bone Marrow Transplant 48:452–458
10. Ando H, Suzuki A, Sakurai S, Kumagai S, Kurita A, Waseda K, Takashima H, Amano T (2017) Tissue characteristics of neointima in late restenosis: integrated backscatter intravascularultrasound analysis for in-stent restenosis. Heart Vessels 32:531–538
11. Hong YJ, Jeong MH, Choi YH, Park SY, Rhew SH, Kim SS, Jeong YW, Jeong HC, Cho JY, Jang SY, Lee KH, Park KH, Sim DS, Yoon NS, Yoon HJ, Kim KH, Park HW, Kim JH, Ahn Y, Cho JG, Park JC (2014) Relation between renal function and neointimal tissue characteristics after drug-eluting stent implantation: virtual histology-intravascular ultrasound analysis. J Cardiol 64:98–104
12. Yonetsu T, Kato K, Kim SJ, Xing L, Jia H, McNulty I, Lee H, Zhang S, Uemura S, Jang Y, Kang SJ, Park SJ, Lee S, Yu B, Kakuta T, Jang IK (2012) Predictors for neoatherosclerosis: a retrospective observational study from the optical coherence tomography registry. Circ Cardiovasc Imaging 5:660–666
13. Muraoka Y, Sonoda S, Kashiyama K, Kamezaki F, Tsuda Y, Araki M, Okazaki M, Otsuji Y (2012) Evaluation of in-stent neointimal tissue components using integrated backscatter intravascularultrasound: comparison of drug-eluting stents and bare-metal stents. Int J Cardiovasc Imaging 28:1635–1641
14. Okura H, Saito Y, Soeda T, Nakao K, Ozaki Y, Kimura K, Ako J, Noguchi T, Yasuda S, Suwa S, Fujimoto K, Nakama Y, Morita T, Shimizu W, Hirohata A, Morita Y, Inoue T, Okamura A, Uematsu M, Hirata K, Tanabe K, Shibata Y, Owa M, Tsujita K, Nishimura K, Miyamoto Y, Ishihara M, J-MINUET Investigators (2018) Frequency and prognostic impact of intravascular imaging-guided urgent percutaneous coronary intervention in patients with acute myocardial infarction: results from J-MINUET. Heart Vessels. https://doi.org/10.1007/s00380-018-1285-3
15. Otsuka F, Vorpahl M, Nakano M, Foerst J, Newell JB, Sakakura K, Kutys R, Ladich E, Finn AV, Kolodgie FD, Virmani R (2014) Pathology of second-generation everolimus-eluting stents versus first-generation sirolimus- and paclitaxel-eluting stents in humans. Circulation 129:211–223
16. Nishimoto Y, Ueda Y, Sugihara R, Murakami A, Ueno K, Takeda Y, Hirata A, Kashiwase K, Higuchi Y, Yasumura Y (2017) Comparison of angioscopic findings among second-generation drug-eluting stents. J Cardiol 70:297–302
17. Aoyama T, Ishii H, Toriyama T, Takahashi H, Kasuga H, Murakami R, Amano T, Uetani T, Yasuda Y, Yuzawa Y, Maruyama S, Matsuo S, Matsubara T, Murohara T (2008) Sirolimus-eluting stents vs bare metal stents for coronary intervention in Japanese patients with renal failure on hemodialysis. Circ J 72:56–60